Original Article

Utility of gadoxetate disodium-enhanced magnetic resonance imaging in evaluating liver failure risk after major hepatic resection

Qian-Jun Yu[1#], Yu-Chuan Luo[1#], Zhi-Wei Zuo[2#], Chuan Xie[1], Ting-Yu Yang[1], Tao Wang[1], Long Cheng[1^]

[1]Department of General Surgery, The General Hospital of Western Theater Command, Chengdu, China; [2]Department of Radiology, The General Hospital of Western Theater Command, Chengdu, China

Contributions: (I) Conception and design: QJ Yu, L Cheng, T Wang; (II) Administrative support: L Cheng, T Wang; (III) Provision of study materials or patients: YC Luo, ZW Zuo, C Xie; (IV) Collection and assembly of data: YC Luo, ZW Zuo, C Xie; (V) Data analysis and interpretation: TY Yang; (VI) Manuscript writing: All authors; (VII) Final approval of manuscript: All authors.

[#]These authors contributed equally to this work.

Correspondence to: Long Cheng, MD; Tao Wang, PhD. Department of General Surgery, The General Hospital of Western Theater Command, No. 270 Rongdu Avenue, Jinniu District, Chengdu 610083, China. Email: tmmulong@163.com; taowang6869@126.com.

Background: Post-hepatectomy liver failure (PHLF) is still a predominant cause of hepatectomy-related mortality. However, it is difficult to evaluate the remnant liver functional reserve accurately before surgery to prevent PHLF. In this study, we aimed to explore the role of gadoxetate disodium-enhanced magnetic resonance imaging (MRI) in evaluating remnant liver functional reserve.

Methods: For this cross-sectional study, the sample retrospectively included 56 patients undergoing liver resections of at least three segments between June 2019 and September 2022 at The General Hospital of the Western Theater Command. Pre-surgery assessments involved liver computer tomography (CT), an indocyanine green (ICG) clearance test, the Child-Pugh scoring system, and liver function serum biochemical indicators. Each patient underwent a gadoxetate disodium-enhanced MRI before the hepatectomy, and we measured the remnant hepatocellular uptake index (rHUI) as well as the standard remnant hepatocellular uptake index (SrHUI). We examined the diagnostic utility of rHUI, SrHUI, indocyanine green retention rate of 15 minutes (ICG R15), and Albumin for PHLF. Receiver operating characteristics (ROC) analyses were used to measure the preoperative liver function parameters (namely, rHUI, SrHUI, ICG R15, and Albumin) for predicting PHLF. The areas under the curve (AUCs) were calculated and compared between different preoperative liver function parameters using the Wilson/Brown method. The Pearson or Spearman correlation coefficient was used for correlation analysis between ICG R15, Albumin, and rHUI and between ICG R15, Albumin, and SrHUI, respectively.

Results: Twelve patients (21.43%) had complications of PHLF. We found significant differences in rHUI, SrHUI, ICG R15, and Albumin between the non-PHLF and PHLF groups. The pooled r between ICG R15 and rHUI was −0.591 [95% confidence interval (CI): −0.740 to −0.389, P<0.001], and between ICG R15 and SrHUI was −0.534 (95% CI: −0.703 to −0.308, P<0.001). The area under the curve (AUC) values of rHUI, SrHUI, ICG R15, and Ablumin were 0.871 (sensitivity 81.82%; specificity 91.67%), 0.878 (sensitivity 79.55%; specificity 83.33%), 0.835 (sensitivity 99.73%; specificity 66.67%), and 0.782 (sensitivity 88.64%; specificity 58.33%), respectively.

Conclusions: We found that the rHUI and SrHUI calculated using the gadoxetate disodium-enhanced MRI reflected a combination of remnant hepatocyte function and liver volume, and these were useful as a quantitative assessment indicator of remnant liver functional reserve and can be a better predictor of PHLF

^ ORCID: 0009-0002-2563-1442.

after major hepatic resection.

Keywords: Gadoxetate disodi; liver function; major hepatectomy; post-hepatectomy liver failure (PHLF)

Submitted Oct 25, 2023. Accepted for publication Mar 18, 2024. Published online Apr 26, 2024.
doi: 10.21037/qims-23-1504
View this article at: https://dx.doi.org/10.21037/qims-23-1504

Introduction

Advances in surgical procedures have made a partial liver resection of any of the liver segments possible. However, major hepatectomy is typically accompanied by a risk of post-hepatectomy liver failure (PHLF) (1). The detailed criteria of PHLF include a higher value of the international normalized ratio (INR) 5 or more days after the operation, or the need for an intravenous injection of fresh frozen plasma to maintain a normal INR accompanied by hyperbilirubinemia (according to the normal cut-off levels defined by the local laboratory) (2). The primary causes of PHLF include the small volume and damage of liver function post liver resection. The incidence of PHLF in the literature varies between 1.2% and 32% partly as a result of differences in the studied patient populations and performed procedures (3,4). PHLF remains a major concern and has been shown to be a predominant cause of hepatectomy-related mortality (5). Therefore, it is important to evaluate the remnant liver functional reserve prior to surgery. The methods that are in use currently, such as liver function serum biochemical indices, the Child-Pugh scoring system, and liver volumetry, do not provide an accurate assessment of the liver function before hepatectomy (6). The indocyanine green retention rate of 15 minutes (ICG R15) is another indicator that is extensively used to evaluate the preoperative liver reserve function. However, the ICG R15 too is not free from limitations (7). A common disadvantage of these methods is that they provide a preoperative assessment of liver function for the liver as a whole, not regionally. However, the challenge in evaluating the pathological status is that liver cell functions may appear heterogeneous among different areas, especially in diseased livers (8). Therefore, evaluating liver function in the different segments becomes critical for a precise assessment of the remnant liver functional reserve.

Gadoxetate disodium is a magnetic resonance imaging (MRI) contrast agent with hepatobiliary specificity. After intravenous injection of gadoxetate disodium, half of the dosage is absorbed by the hepatic cells through organic anion transport proteins. Following that, it is discharged into the biliary tract via multidrug resistance proteins on the bile capillaries without entering the enterohepatic circulation or reabsorption, and the other 50% of the gadoxetate disodium is excreted via the kidneys. Approximately 20 minutes after being injected intravenously, it enters a hepatobiliary-specific phase that lasts for 2 hours (9). The uptake ability of hepatic cells for gadoxetate disodium has been found to be positively correlated with hepatocyte function (10-12). Furthermore, gadoxetate disodium-enhanced MRI can accurately detect regional liver function by measuring relevant indicators (8,13,14). Therefore, there are potential advantages for using gadoxetate disodium-enhanced MRI examinations for evaluating the remnant liver functional reserve more precisely.

Based on these findings, we aimed to evaluate remnant liver functional reserve using gadoxetate disodium-enhanced MRI and analyze its value in predicting the risk of PHLF after major hepatectomy. We present this article in accordance with the STROBE reporting checklist (available at https://qims.amegroups.com/article/view/10.21037/qims-23-1504/rc).

Methods

Study participants

In this retrospective study, we collected all data from patients in accordance with the ethical principles of the World Medical Association specified in the Declaration of Helsinki (as revised in 2013). The study was approved by the Ethics Committee of the General Hospital of Western Theater Command (No. XZLL-20170087). Written informed consent was obtained from all participants. Our study sample included 56 patients who underwent major hepatectomy at The General Hospital of the Western Theater Command, China, between June 2019 and September 2022 (*Figure 1*). These patients suffered from hepatocellular carcinoma, intrahepatic cholangiocarcinoma, hepatic hemangioma, or intrahepatic bile duct stones. The

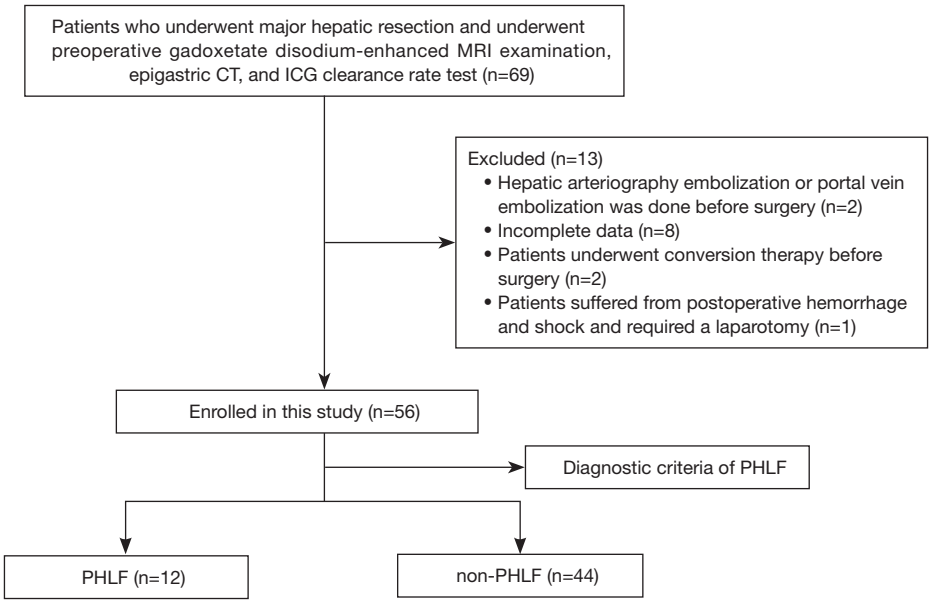

Figure 1 Patient selection flowchart. MRI, magnetic resonance imaging; CT, computed tomography; ICG, indocyanine green; PHLF, post-hepatectomy liver failure.

surgery of these patients followed the relevant treatment guidelines and expert consensus (15). Among these patients, there were 41 males and 15 females with an average age of 53.05±9.78, ranging from 35 to 77 years. Within this sample, 32 males and 12 females, with an average age of 52.68±8.69 years, were categorized into the non-PHLF group, while 9 males and 3 females, with an average age of 54.41±10.56 years, were classified into the PHLF group.

Inclusion criteria: (I) patients who underwent gadoxetate disodium-enhanced MRI examination and major hepatectomy; (II) patients on whom gadoxetate disodium-enhanced MRI examination and liver enhanced computer tomography (CT) were performed within four weeks prior to the surgery; and (III) a liver function test and an ICG clearance rate test were completed within one week before the operation. Exclusion criteria: (I) patients less than 18 years old; (II) pregnant women; and (III) patients who had received selective hepatic arteriography embolization, radiotherapy, or chemotherapy prior to the surgery.

Major hepatic resection was defined as a resection including three or more segments, based on the Couinaud classification (16). For the diagnostic criteria of PHLF, we referred to the criteria proposed by the International Study Group of Liver Surgery (ISGLS) in 2011 (2). The detailed criteria included a higher value of the INR five or more days after the surgery or the need for an intravenous injection of fresh frozen plasma to maintain a normal INR accompanied by hyperbilirubinemia (as per the normal cut-off levels defined by the local laboratory).

MRI and CT examination procedures

MRI

We used a Siemens Avanto 1.5 T MRI scanner with a body-phased array coil for all the MRI examinations. The patient was placed in the supine position so that the midsection, including the entire liver and spleen, could be scanned. The enhanced scanning dynamic period included the arterial phase and the hepatobiliary phase. The scanning time was 20 s to 20 minutes after the contrast agent was administered. The contrast agent used was gadoxetate disodium at a dosage of 0.025 mmol/kg and an injection flow rate of 2 mL/s. Then, after injecting the contrast agent, 20 mL of normal saline was immediately injected at the same rate to flush the vein.

Scanning sequence and parameters: (I) axial T2WI, time of repetition (TR) =1,100 ms, time of echo (TE) =74 ms, field of view (FOV) =370×370, slice thickness =6 mm; (II) axial T1WI, TR =113 ms, TE =4.91 ms, FOV =370×370, slice thickness =6 mm; (III) diffusion weighted imaging (DWI) b-factors 0, 50, 600, TR =2,400 ms, TE =75 ms, FOV =370×370, slice thickness =6 mm;

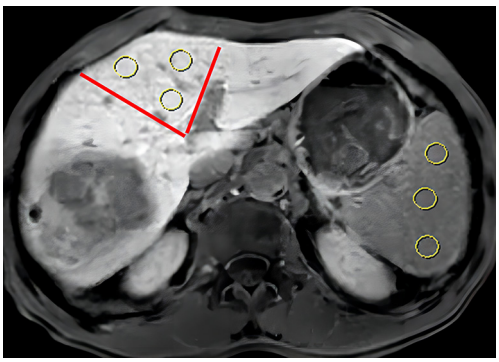

Figure 2 Calculation of the ROI mean signal intensity using liver segment (S4) and spleen ROI in the hepatobiliary-specific period via gadoxetate disodium-enhanced MRI. The area of the red line indicates the liver segment. Yellow circles indicate ROI. MRI, magnetic resonance imaging; ROI, region of interest.

(IV) coronal T2WI, TR =1,200 ms, TE =93 ms, FOV =380 ×380, slice thickness =6 mm; (V) three-dimensional T1-weighted gradient echo sequence (volumetric interpolated breath-hold examination, VIBE) with the fat-suppression technique, TR =5 ms, TE =2 ms, FOV =370×370, slice thickness =3 mm.

For the enhanced scanning arterial phase, scanning was started 20 s after the contrast agent was injected, and for the hepatobiliary-specific period, scanning was started 20 minutes after the injection of the contrast agent.

CT

We used a Toshiba Aquilion One 320-row spiral CT. Patients were fasting for 6 to 12 hours prior to the examination and were instructed to avoid strenuous exercise 30 minutes prior to the examination. The scanning parameters were as follows: tube voltage 120 kV; self-motion tube current (automatic adjustment was made according to the thickness of the body); rotation time for one circle of the CT bulb tube was 0.5 s; screw pitch 87 mm; Pitca Factor/Helical 0.5×100, FOV 350×350 mm, matrix 512×512; and the scanning area ranged from the diaphragmatic dome to the inferior margin of the liver, encompassing the entire liver. Three-phase enhanced scanning was carried out with the same parameters as above.

Quantitative analysis using the gadoxetate disodium-enhanced MRI

We measured the hepatocellular uptake index (HUI) from the liver volume (*V*) and mean signal intensity of the liver segments on contrast-enhanced T1-weighted images with fat suppression (*L20*) and mean signal intensity of the spleen on contrast-enhanced T1-weighted images with fat suppression (*S20*) on a 2D gradient-echo T1-weighted images with fat suppression at 20 minutes after gadoxetate disodium (0.025 mmol/kg of body weight) administration. These were determined using the following equation (17): $V\,[(L20/S20)-1]$.

We used the following computational formula to calculate the HUI of the remnant liver: rHUI = $rV[(rL20/S20)-1]$, where rHUI refers to the remnant hepatocellular uptake index, *rV* refers to the remnant liver volume, and rL20 is the mean signal intensity of the remnant liver segments during the MR hepatobiliary-specific period 20 minutes after gadoxetate disodium was administered intravenously. To standardize the rHUI, we used the following formula that takes into consideration the patients' body surface area: SrHUI = rHUI/SA, where SrHUI refers to the standard remnant hepatocellular uptake index and SA is the surface area.

Segment L20 measurement (*Figure 2*): an experienced radiology physician and an experienced hepatological surgeon analyzed the gadoxetate disodium-enhanced MR images. We used the INFINITT CDViewer film reading tool to calculate the region of interest (ROI) mean signal intensity of the remnant liver segment of the liver parenchyma, but the focal lesions were not measured. The same method was used to calculate the mean signal intensity of the spleen parenchyma. The selection of ROI: the observers placed the ROI box in one to three different regions in the main layer of each remnant liver segment to calculate the mean signal intensity of the remnant liver. To reduce errors, the area of every ROI was 1–2 cm^2 to avoid including biliary ducts, blood vessels, and other prominent artifacts.

Measurement of liver segment volume (*Figure 3*): the patients' enhanced CT images were imported into the Myrian liver three-dimensional (3D) surgical planning system. Then, the portal veins were marked layer by layer, and the major portal vein branches were created by the system. When a segment of a portal vein branch was marked (*Figure 3A*), the relative liver segment volume was generated automatically by the system (*Figure 3B*). Accordingly, by marking every liver segment portal vein (*Figure 3C*), the volumes of all of the relative liver segments were calculated using the same method (*Figure 3D*).

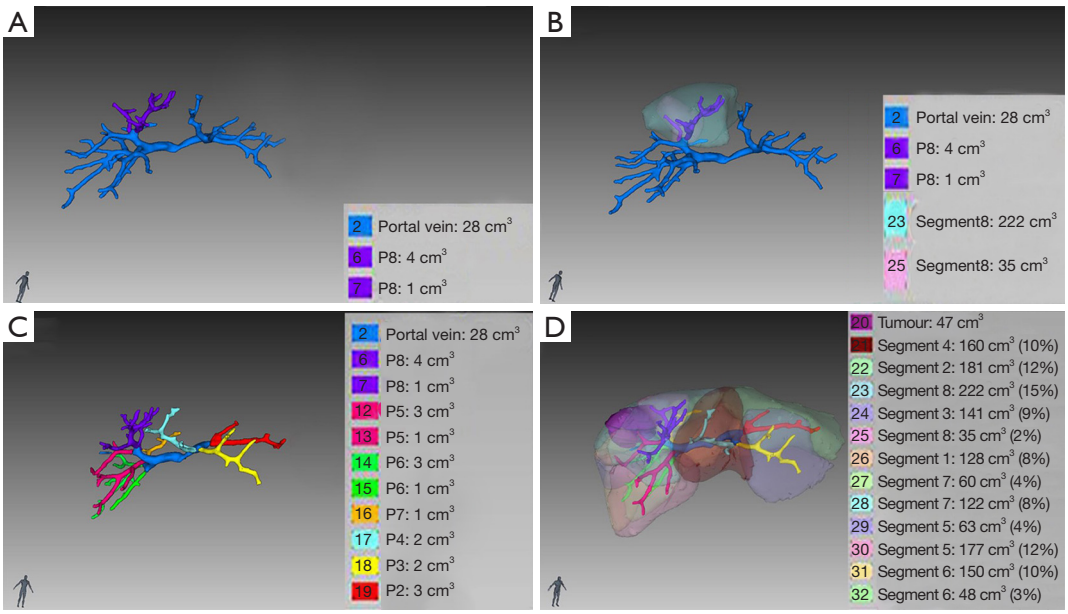

Figure 3 Use of the Myrian liver 3D surgical planning system to calculate regions and liver segment volumes. (A) A segment portal vein branch is marked; (B) the marked liver segment volume is formed automatically; (C) every liver segment portal vein branch is marked; (D) all the liver segment volumes are calculated automatically. Lilac indicates lesions. 3D, three-dimensional.

Hepatic function parameters

In this study, we measured the following hepatic function parameters preoperatively (within a week) and postoperatively (within 24 hours): alanine aminotransferase (ALT), aspartate transaminase (AST), alkaline phosphatase (ALP), INR, prothrombin time (PT), gamma-glutamyl transpeptidase (GGT), total bilirubin (TBIL), Albumin, creatinine (Cre), platelet (PLT), and prealbumin; the Child-Pugh score was also calculated and recorded. Preoperative ICG R15 was measured using the following procedure: After an overnight fast, ICG at a dose of 0.5 mg/kg was given as an intravenous bolus through a peripheral vein. Blood samples were collected at 5, 10, and 15 minutes, and the plasma ICG concentration was measured spectrophotometrically. The ICG R15 was calculated and recorded.

Liver resection and perioperative treatments

The surgery plan was developed based on each patient's preoperative Child-Pugh score, ICG R15, liver MRI, liver CT, and 3D reconstruction, as well as the standard liver volume. We referred to the Consensus on Evaluation of Hepatic Functional Reserve before Hepatectomy (2011) (16) for determining the area and range of the hepatectomy, and the final surgery plan was adjusted based on the specific conditions during the operation. Based on the conditions found during the surgery, the surgeon decided whether or not to conduct the first hepatic portal control. If it was so, then the Pringle maneuver was adopted. The laparotomy procedures for all patients involved a combination of an ultrasound knife, an electrotome, and a cutting stapling device to complete the hepatectomy.

Based on the serum TBIL and INR normal values defined by The General Hospital of Western Theater Command, the following symptoms appearing five days after hepatectomy were considered postoperative combined hepatic failure risk: INR >1.20 that was maintained only with intravenous injection of fresh frozen plasma and TBIL >28.0 μmol/L. If abnormal liver function was detected prior to the surgery, we included the preoperative abnormal results for analyzing the measurements and evaluation. In this study, one patient suffered from postoperative hemorrhage and shock and required a laparotomy; hence, we excluded this case from the data analysis and it was not included in the total sample size of 56 cases. We also recorded the surgery time and the amount of bleeding during the surgery. All the patients who underwent hepatectomy were routinely shifted to the intensive care unit of the department.

Statistical analysis

We used Graphpad Prism 8.0.1 for statistical analysis. Categorical variables were described using percentages (counts), and we compared the differences in categorical variables between groups using the Chi-squared test. Continuous variables were described using the mean and standard deviation, and the differences in continuous variables between groups were compared using an independent Student's *t*-test or the Mann-Whitney *U* test. The normality of the variables was verified by the Kolmogorov-Smirnov test. If so, the Student's *t*-test was used. If not, the MANN-Whitney *U* test was used. Receiver operating characteristics (ROC) analyses were used to measure the preoperative liver function parameters (namely, rHUI, SrHUI, ICG R15, and Albumin) for predicting PHLF. The areas under the curve (AUCs) were calculated and compared between different preoperative liver function parameters using the Wilson/Brown method. The Pearson or Spearman correlation coefficient was used for correlation analysis between ICG R15, albumin, and rHUI and between ICG R15, albumin, and SrHUI, respectively. A two-tailed P value of < 0.05 was considered statistical significance.

Results

Overview of general health status

The preoperative general health status of patients in our study is shown in *Table 1*. There were 56 patients who underwent the following major hepatic resections: 28 underwent a left lobectomy, 25 underwent a right lobectomy, and 3 underwent a left extended lobectomy. Among the 56 patients with major hepatectomy, 12 patients (21.43%) experienced PHLF, and there were no deaths. There were 36 patients with hepatocellular carcinoma, 6 patients with intrahepatic cholangiocarcinoma, 10 patients with hepatic hemangioma, 3 patients with calculus of the intrahepatic duct, and 1 patient with hepatitis granuloma.

There were differences in the liver gadoxetate disodium-enhanced MRI signal intensity among patients without either hepatitis B or liver cirrhosis, patients with hepatitis B but without liver cirrhosis, and patients with both hepatitis B and liver cirrhosis (*Figure 4*). Among patients with liver cirrhosis, we found that the different liver segments showed variations in the gadoxetate disodium-enhanced MRI signal intensity (*Figure 5*).

Comparison of relative indicators between the non-PHLF and PHLF groups

We used the Mann-Whitney *U* test or the independent Student's *t*-test to analyze these various indicators (*Table 1*) and found that there were significant differences between the non-PHLF and PHLF groups in the levels of rHUI, SrHUI, ICG R15, and Albumin ($P<0.001$, $P<0.001$, $P=0.002$, and $P=0.002$, respectively). The pooled r between ICG R15, Albumin, and rHUI was –0.591 [95% confidence interval (CI): –0.740 to –0.389, $P<0.001$], 0.515 (95% CI: 0.291 to 0.685, $P<0.001$), and between ICG R15, Albumin, and SrHUI was –0.534 (95% CI: –0.703 to –0.308, $P<0.001$), 0.492 (95% CI: 0.255 to 0.673, $P=0.001$) (*Figure 6*). There were no significant differences in any other indicators, namely, ALP, GGT, AST, ALT, TBIL, PLT, and remnant liver volume.

rHUI and SrHUI had better diagnostic value in predicting post-hepatectomy hepatic failure

We utilized ROC curves to analyze the diagnostic accuracy of HUI in evaluating PHLF risk. The AUCs of rHUI, SrHUI, ICG R15, and Albumin were 0.871 (sensitivity 81.82%, specificity 91.67%, cut-off value: 0.633 L; 95% CI: 0.777–0.966), 0.878 (sensitivity 79.55%, specificity 83.33%, cut-off value: 0.386 L/m^2; 95% CI: 0.773–0.982), 0.835 (sensitivity 99.73%, specificity 66.67%, cut-off value: 10.45%; 95% CI: 0.673–0.997), and 0.782 (sensitivity 88.64%, specificity 58.33%, cut-off value: 39.2 g/L; 95% CI: 0.634–0.930), respectively (*Table 2*, *Figure 7*). The Youden index was calculated as sensitivity + specificity –1. The result corresponding to the maximum value of the Youden index was the cut-off value.

Discussion

PHLF has a high incidence and mortality rate and is also one of the challenging complications that prolongs the duration of hospital stays and significantly increases costs for patients (18-20). To prevent the occurrence of PHLF, precise quantification when evaluating the remnant liver functional reserve is invaluable. Frequently used methods for evaluating liver reserve function include liver function serum biochemical indices and the Child-Pugh score, but these do not predict PHLF accurately (8,21). ICG R15 and liver volume measurement have also been extensively utilized, and among these, ICG R15 has gained widespread

Table 1 The differences of patients' clinical indices between the non-PHLF and PHLF groups

Clinical indices	Non-PHLF (n=44)	PHLF (n=12)	P value
General conditions			
Sex (man)	32 (72.73)	9 (75.00)	0.87
Age (years)	53.57±9.59	51.17±9.65	0.45
Hepatitis	34 (77.27)	10 (83.33)	0.65
Cirrhosis	30 (68.18)	8 (66.67)	0.92
Pre-operation			
ALT (U/L)	34.04±10.28	32.14±10.63	0.57
AST (U/L)	33.21±10.09	35.31±13.44	0.55
ALP (U/L)	72.76±17.39	79.02±12.07	0.24
GGT (U/L)	57.83±24.50	72.80±25.67	0.06
TBIL (mmol/L)	26.91±8.60	28.89±9.44	0.42
Albumin (g/L)	42.85±3.29	39.42±3.09	0.002
PT (S)	11.57±1.30	11.85±1.16	0.33
PLT (10^9/L)	168.80±37.43	172.50±62.44	0.74
Creatinine (μmol/L)	54.43±15.95	65.71±35.37	0.36
Pre-albumin (mg/L)	188.70±19.47	176.10±25.54	0.06
Child-Pugh score			0.06
A5	39 (88.64)	8 (66.67)	
A6	5 (11.36)	4 (33.33)	
RLV (mL)	571.60±88.91	515.80±88.24	0.05
ICG R15 (%)	6.10±2.60	11.00±4.30	0.002
rHUI (L)	0.895±0.30	0.524±0.12	<0.001
SrHUI (L/m^2)	0.615±0.24	0.347±0.09	<0.001
Intra-operation			
Blood loss (mL)	378.20±88.61	401.70±89.22	0.42
Operation time (min)	264.50±42.04	280.70±56.25	0.22

Values are presented as mean ± SD or number (%). PHLF, post-hepatectomy liver failure; ALT, alanine aminotransferase; AST, aspartate transaminase; ALP, alkaline phosphatase; GGT, gamma-glutamyl transferase; TBIL, total bilirubin; PT, prothrombin time; PLT, platelet; RLV, remnant liver volume; ICG R15, indocyanine green retention test; rHUI, remnant hepatocellular uptake index; SrHUI, standard remnant hepatocellular uptake index.

acceptability in assessing liver reserve function.

However, in some patients with hepatic cirrhosis, liver function is heterogeneously distributed among the different liver lobes or segments (10,12). In these situations, these two methods cannot provide precise results in the quantitative evaluation of postoperative remnant liver function. For a successful hepatectomy, an accurate preoperative evaluation of the liver resection area and range is essential for planning the surgery. While removing the focal lesions, it is very important to ensure that the risk of PHLF is minimized as much as possible. Therefore, an evaluation method that can aid in precise quantification in conjunction with remnant hepatic cell function and remnant liver volume can be extremely valuable in improving the accuracy of predicting PHLF.

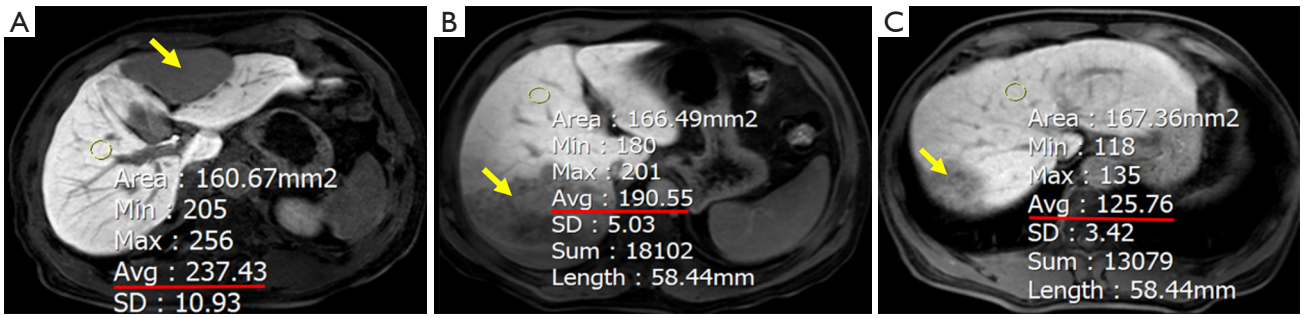

Figure 4 Varied hepatopathy and different gadoxetate disodium-enhanced MRI signal intensity: (A) male, 54 years old, hepatic hemangioma (yellow arrow), ROI (yellow circle): 237.43; (B) male, 48 years old, hepatitis B, intrahepatic cholangiocarcinoma (yellow arrow), ROI (yellow circle): 190.55, (C) male, 60 years old, hepatitis B, cirrhosis, hepatocellular carcinoma (yellow arrow), ROI (yellow circle): 125.76. Avg, average; SD, standard deviation; MRI, magnetic resonance imaging; ROI, region of interest.

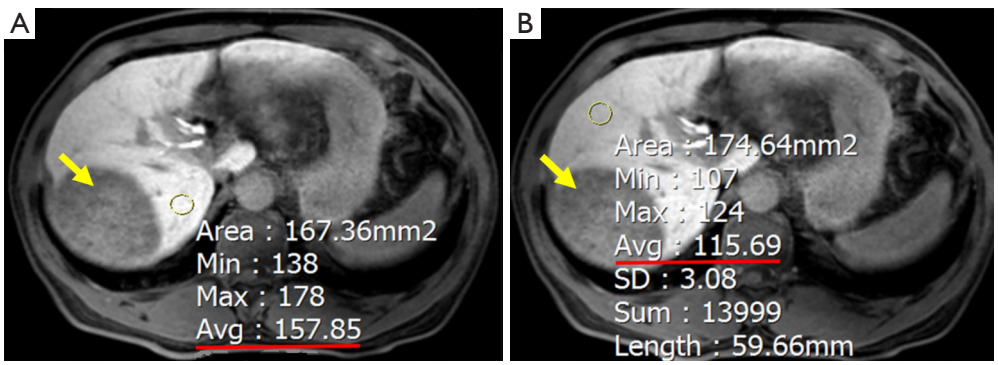

Figure 5 Comparison of the gadoxetate disodium-enhanced MRI signal intensity in different regions and segments of livers with cirrhosis: (A) and (B) are of the same patient: male, 60 years old, hepatitis B, liver cirrhosis, hepatocellular carcinoma (yellow arrow). (A) ROI (yellow circle): 157.85; (B) ROI (yellow circle): 115.69. Avg, average; SD, standard deviation; MRI, magnetic resonance imaging; ROI, region of interest.

In this study, we used the computational formula for evaluating the liver reserve function index HUI mentioned by Yamada *et al.* (17), where [(*rL20/S20*)–1] represents the remnant liver cell function; incorporating spleen signal intensity (S20) helps to verify the influence of the gadoxetate disodium dose on its distribution in the extracellular space; and *rV* represents the volume of the remnant liver. rHUI has the advantages of combining remnant hepatocyte functions and volume to jointly evaluate liver function and, hence, may be able to quantify the remnant liver functional reserve more precisely (20,22,23).

In this study, among the various indicators that we evaluated to predict the risk of PHLF, we found statistically significant differences between the non-PHLF and PHLF groups with regard to rHUI, SrHUI, ICG R15, and albumin. Yoon *et al.* (24) noted that ICG R15 is the indicator that is most frequently used in surgical candidates to assess their functional reserve and to determine the extent of surgery (25-27). In our study, we found that rHUI, SrHUI, and ICG R15 were significantly correlated (r=–0.591, P<0.001; r=–0.534, P<0.001). Furthermore, rHUI and SrHUI had a larger AUC (0.871 and 0878, respectively) when compared to ICG R15 (0.835) and ablumin (0.782) (all P<0.001). This indicates that rHUI and SrHUI were superior to ICG R15, the Child-Pugh score, and the liver function serum index in predicting PHLF in this study.

The ICG R15 provides a relatively precise quantification when evaluating the functioning of the liver as a whole, but it is limited in its ability to evaluate regional liver functions. The findings of this study reveal that both rHUI and SrHUI offer distinct advantages over traditional indicators such as ICG R15, Child-Pugh

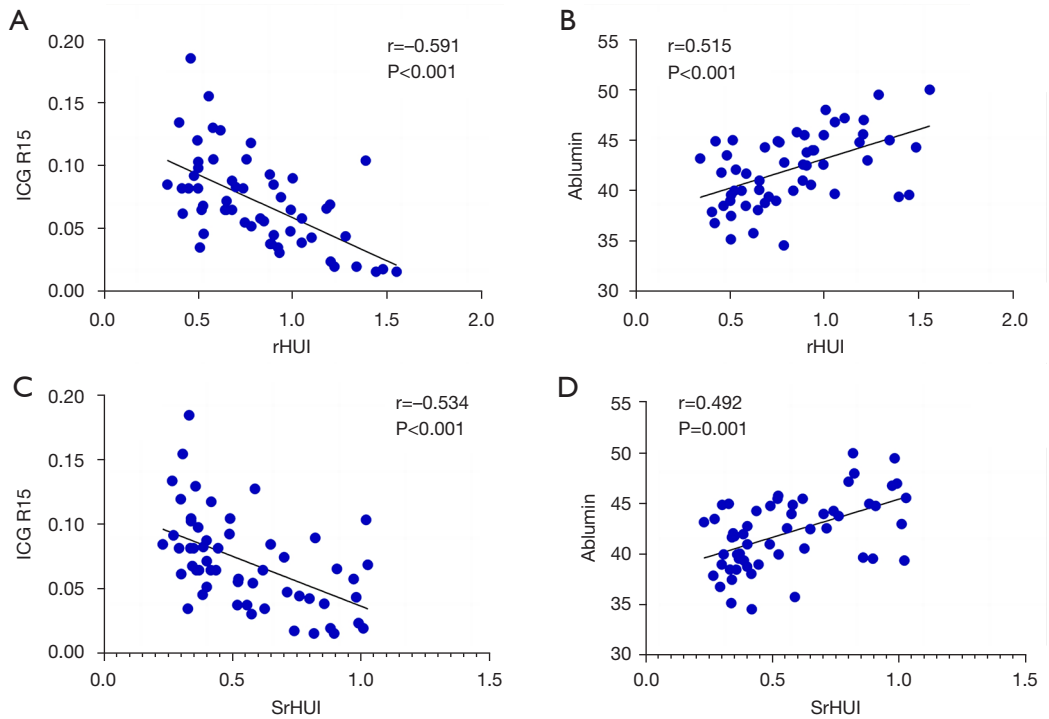

Figure 6 rHUI and SrHUI were significantly correlated with ICG R15 and albumin, respectively. (A) The pooled r between ICG R15 and rHUI was –0.591 (95% CI: –0.740 to –0.389, P<0.001). (B) The pooled r between ablumin and rHUI was 0.515 (95% CI: 0.291 to 0.685, P<0.001). (C) The pooled r between ICG R15 and SrHUI was –0.534 (95% CI: –0.703 to –0.308, P<0.001). (D) The pooled r between ablumin and SrHUI was 0.492 (95% CI: 0.255 to 0.673, P=0.001). ICG R15, indocyanine green retention rate in 15 minutes; rHUI, remnant hepatocellular uptake index; SrHUI, standard remnant hepatocellular uptake index; CI: confidence interval.

Table 2 AUC and cut-off value for rHUI, SrHUI, ICG R15, and albumin in ROC analyses in predicting PHLF

Preoperative indices	Cut-off value	AUC (95% CI)	P value
rHUI (L)	0.633	0.871 (0.777–0.966)	<0.001
SrHUI (L/m^2)	0.386	0.878 (0.773–0.982)	<0.001
ICG R15 (%)	10.45	0.835 (0.673–0.997)	<0.001
Ablumin (g/L)	39.2	0.782 (0.634–0.930)	0.002

AUC, area under the curve; rHUI, remnant hepatocellular uptake index; SrHUI, standard remnant hepatocellular uptake index; ICG R15, indocyanine green retention rate in 15 minutes; ROC, receiver operating characteristic; PHLF, post-hepatectomy liver failure; CI, confidence interval.

score, and albumin levels when predicting PHLF risk preoperatively. Notably, these advantages stem from their dual capability to assess remnant liver functional reserve in conjunction with both remnant liver cell function and volume, as well as their capacity to quantitatively evaluate liver function across various liver regions. It is imperative to acknowledge, however, that the limited sample size employed in this study may have led to type II errors during the statistical analysis process, as noted in previous literature (28). Consequently, a meticulous and objective elaboration of this aspect is essential to ensure a comprehensive understanding of the study's implications.

In this study, the levels of albumin, a marker of liver synthesis function, were significantly different between the non-PHLF and PHLF groups, and its AUC was 0.782, indicating that albumin is of importance in evaluating PHLF. However, there was no statistical significance for the Child-Pugh score, which is a combination of albumin,

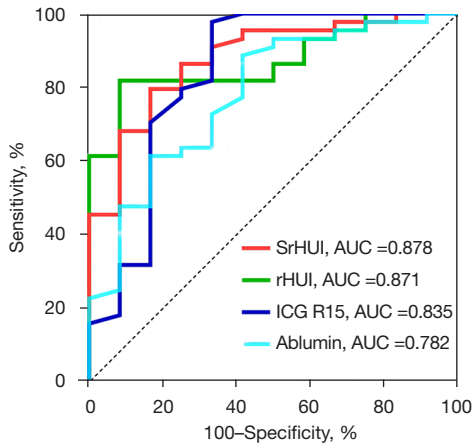

Figure 7 The ROC curves and the AUC for rHUI, SrHUI, ICG R15, and albumin in predicting post-hepatectomy liver failure. SrHUI, standard remnant hepatocellular uptake index; AUC, area under the curve; rHUI, remnant hepatocellular uptake index; ICG R15, indocyanine green retention rate in 15 minutes; ROC, receiver operating characteristic.

bilirubin, PT, ascites, and hepatic encephalopathy. These two results are not inconsistent, as this study included patients undergoing major hepatectomy, and to ensure that the surgery was safe, patients whose preoperative Child-Pugh scores were all within the normal range were included. As a result, it is understandable that there were no significant differences in the Child-Pugh scores (P=0.06) between the non-PHLF and PHLF groups.

At present, most liver function evaluation methods are done under the assumption that liver function is evenly distributed across the entire liver (29,30). However, studies have demonstrated pathological evidence for variations among different regions of the liver (8,31). In this study, we found obvious differences in the hepatocyte uptake amount of gadoxetate disodium among patients with varied hepatopathy (*Figure 4*). Breit *et al.* showed similar results, stating that mean Gd-concentration in the liver parenchyma was significantly higher for healthy patients than for those with liver fibrosis or cirrhosis and with acute liver disease (32). Furthermore, there was an uneven distribution in the uptake amount of gadoxetate disodium in different hepatic cirrhosis regions. These confirm that liver function is distributed heterogeneously in patients with hepatic cirrhosis (*Figure 5*). There are also reports (9,12) indicating that gadoxetate disodium-enhanced MRI can be used to evaluate regional variations in liver function.

There are some deficiencies in this study. First, this is a primary retrospective study with a small sample size. The results of this study suggest that for patients assessed preoperatively as being at greater risk of PHLF, the volume of the reserved liver can be corrected by preoperative medications to correct hepatocellular function or increased by means of portal vein embolization or associated liver partition and portal vein ligation for staged hepatectomy (ALPPS) procedures. In order to obtain more reliable research results, further research should incorporate a larger sample size as well as comparing different levels of severity of PHLF. Second, the preoperative serum TBIL of patients included in this study was mostly within the normal range. However, in clinical practice, an obvious elevation of bilirubin is a common finding among many patients with hepatic calculus and portal hepatic carcinoma. The metabolism of gadoxetate disodium and bilirubin is roughly similar, and the two compete for the same carrier. Given this situation, the evaluation of preoperative hepatic reserve function via gadoxetate disodium-enhanced MRI should be interpreted prudently. Third, the approach is that the results are highly dependent on the imaging protocol (e.g., flip angle), field strength, and likely vendor. While this is probably feasible for a single center with a highly controlled protocol at a single field strength, these results are probably not generalizable. A better strategy might be the use of T1 mapping methods that should be less dependent on protocol and vendor (although still dependent on field strength). Fourth, the measurement of the signal intensity of gadoxetate disodium-enhanced MR images was performed by a radiologist and a hepatobiliary surgeon. Both should be checked for consistency after completing their respective measurements, so that the results can be more accurate. Furthermore, serum albumin and ICG R15 were lower in the preoperative PHLF group than in the non-PHLF pre-operatively, possibly implying poorer liver function in the preoperative PHLF group. However, there were no statistically significant differences in other indicators representing liver function. These results make the preoperative situation of liver function superiority and inferiority in the two groups unclear and complicate the interpretation of the study results.

Conclusions

In conclusion, we found that rHUI is a favorable index that

combines remnant liver cell function and volume to evaluate remnant liver functional reserve. Gadoxetate disodium-enhanced MRI is effective in accurately measuring the liver regional reserve in different segments of the liver. Therefore, gadoxetate disodium-enhanced MRI has the potential to predict PHLF after major hepatectomy.

Acknowledgments

We are particularly grateful to all the people who have given us help on our article.
Funding: This study was supported by the Natural Science Foundation of Sichuan Province (No. 2022NSFSC0610) and the Youth Foundation of Science and Technology Department of Sichuan Province (No. 2016JQ0023).

Footnote

Reporting Checklist: The authors have completed the STROBE reporting checklist. Available at https://qims.amegroups.com/article/view/10.21037/qims-23-1504/rc

Conflicts of Interest: All authors have completed the ICMJE uniform disclosure form (available at https://qims.amegroups.com/article/view/10.21037/qims-23-1504/coif). The authors have no conflicts of interest to declare.

Ethical Statement: The authors are accountable for all aspects of the work in ensuring that questions related to the accuracy or integrity of any part of the work are appropriately investigated and resolved. The study was conducted in accordance with the Declaration of Helsinki (as revised in 2013). The study was approved by the Ethics Committee of the General Hospital of Western Theater Command (No. XZLL-20170087). Written informed consent was obtained from all participants.

References

1. Eshkenazy R, Dreznik Y, Lahat E, Zakai BB, Zendel A, Ariche A. Small for size liver remnant following resection: prevention and management. Hepatobiliary Surg Nutr 2014;3:303-12.
2. Rahbari NN, Garden OJ, Padbury R, Brooke-Smith M, Crawford M, Adam R, et al. Posthepatectomy liver failure: a definition and grading by the International Study Group of Liver Surgery (ISGLS). Surgery 2011;149:713-24.
3. Kawano Y, Sasaki A, Kai S, Endo Y, Iwaki K, Uchida H, Shibata K, Ohta M, Kitano S. Short- and long-term outcomes after hepatic resection for hepatocellular carcinoma with concomitant esophageal varices in patients with cirrhosis. Ann Surg Oncol 2008;15:1670-6.
4. Mullen JT, Ribero D, Reddy SK, Donadon M, Zorzi D, Gautam S, Abdalla EK, Curley SA, Capussotti L, Clary BM, Vauthey JN. Hepatic insufficiency and mortality in 1,059 noncirrhotic patients undergoing major hepatectomy. J Am Coll Surg 2007;204:854-62; discussion 862-4.
5. Jarnagin WR, Gonen M, Fong Y, DeMatteo RP, Ben-Porat L, Little S, Corvera C, Weber S, Blumgart LH. Improvement in perioperative outcome after hepatic resection: analysis of 1,803 consecutive cases over the past decade. Ann Surg 2002;236:397-406; discussion 406-7.
6. Hoekstra LT, de Graaf W, Nibourg GA, Heger M, Bennink RJ, Stieger B, van Gulik TM. Physiological and biochemical basis of clinical liver function tests: a review. Ann Surg 2013;257:27-36.
7. Schneider PD. Preoperative assessment of liver function. Surg Clin North Am 2004;84:355-73.
8. Zhou ZP, Long LL, Qiu WJ, Cheng G, Huang LJ, Yang TF, Huang ZK. Evaluating segmental liver function using T1 mapping on Gd-EOB-DTPA-enhanced MRI with a 3.0 Tesla. BMC Med Imaging 2017;17:20.
9. Liang M, Zhao J, Xie B, Li C, Yin X, Cheng L, Wang J, Zhang L. MR liver imaging with Gd-EOB-DTPA: The need for different delay times of the hepatobiliary phase in patients with different liver function. Eur J Radiol 2016;85:546-52.
10. Wibmer A, Prusa AM, Nolz R, Gruenberger T, Schindl M, Ba-Ssalamah A. Liver failure after major liver resection: risk assessment by using preoperative Gadoxetic acid-enhanced 3-T MR imaging. Radiology 2013;269:777-86.
11. Nilsson H, Blomqvist L, Douglas L, Nordell A,

Janczewska I, Näslund E, Jonas E. Gd-EOB-DTPA-enhanced MRI for the assessment of liver function and volume in liver cirrhosis. Br J Radiol 2013;86:20120653.
12. Li L, Tang H, Liu Y, Lin L, Chen G, Cai L, Yuan F, Song B. Evaluation of hepatic functional reserve on Gd-EOB-DTPA-enhanced MRI. Radiologic Practice 2016;31:19-25.
13. Wang Y, Zhang L, Ning J, Zhang X, Li X, Zhang L, Chen G, Zhao X, Wang X, Yang S, Yuan C, Dong J, Chen H. Preoperative Remnant Liver Function Evaluation Using a Routine Clinical Dynamic Gd-EOB-DTPA-Enhanced MRI Protocol in Patients with Hepatocellular Carcinoma. Ann Surg Oncol 2021;28:3672-82.
14. Araki K, Harimoto N, Yamanaka T, Ishii N, Tsukagoshi M, Igarashi T, Watanabe A, Kubo N, Tsushima Y, Shirabe K. Efficiency of regional functional liver volume assessment using Gd-EOB-DTPA-enhanced magnetic resonance imaging for hepatocellular carcinoma with portal vein tumor thrombus. Surg Today 2020;50:1496-506.
15. Lang BH, Poon RT, Fan ST, Wong J. Perioperative and long-term outcome of major hepatic resection for small solitary hepatocellular carcinoma in patients with cirrhosis. Arch Surg 2003;138:1207-13.
16. Dong JH, Zheng SS, Chen XP, Dou KF, Fan J, Bie P, Geng XP, Lv WP. Consensus on evaluation of Hepatic functional reserve before hepatectomy (2011 edition). Chin J Dig Surg 2011;10:20-5.
17. Yamada A, Hara T, Li F, Fujinaga Y, Ueda K, Kadoya M, Doi K. Quantitative evaluation of liver function with use of gadoxetate disodium-enhanced MR imaging. Radiology 2011;260:727-33.
18. van den Broek MA, Olde Damink SW, Dejong CH, Lang H, Malagó M, Jalan R, Saner FH. Liver failure after partial hepatic resection: definition, pathophysiology, risk factors and treatment. Liver Int 2008;28:767-80.
19. Lock JF, Reinhold T, Malinowski M, Pratschke J, Neuhaus P, Stockmann M. The costs of postoperative liver failure and the economic impact of liver function capacity after extended liver resection--a single-center experience. Langenbecks Arch Surg 2009;394:1047-56.
20. Geisel D, Raabe P, Lüdemann L, Malinowski M, Stockmann M, Seehofer D, Pratschke J, Hamm B, Denecke T. Gd-EOB-DTPA-enhanced MRI for monitoring future liver remnant function after portal vein embolization and extended hemihepatectomy: A prospective trial. Eur Radiol 2017;27:3080-7.
21. Kukuk GM, Schaefer SG, Fimmers R, Hadizadeh DR, Ezziddin S, Spengler U, Schild HH, Willinek WA. Hepatobiliary magnetic resonance imaging in patients with liver disease: correlation of liver enhancement with biochemical liver function tests. Eur Radiol 2014;24:2482-90.
22. Park HJ, Yoon JS, Lee SS, Suk HI, Park B, Sung YS, Hong SB, Ryu H. Deep Learning-Based Assessment of Functional Liver Capacity Using Gadoxetic Acid-Enhanced Hepatobiliary Phase MRI. Korean J Radiol 2022;23:720-31.
23. Akabane M, Shindoh J, Kobayashi Y, Okubo S, Matsumura M, Hashimoto M. Risk Stratification of Patients with Marginal Hepatic Functional Reserve Using the Remnant Hepatocyte Uptake Index in Gadoxetic Acid-Enhanced Magnetic Resonance Imaging for Safe Liver Surgery. World J Surg 2023;47:1042-8.
24. Yoon JH, Lee JM, Kang HJ, Ahn SJ, Yang H, Kim E, Okuaki T, Han JK. Quantitative Assessment of Liver Function by Using Gadoxetic Acid-enhanced MRI: Hepatocyte Uptake Ratio. Radiology 2019;290:125-33.
25. Lee SG, Hwang S. How I do it: assessment of hepatic functional reserve for indication of hepatic resection. J Hepatobiliary Pancreat Surg 2005;12:38-43.
26. Lau H, Man K, Fan ST, Yu WC, Lo CM, Wong J. Evaluation of preoperative hepatic function in patients with hepatocellular carcinoma undergoing hepatectomy. Br J Surg 1997;84:1255-9.
27. Hemming AW, Scudamore CH, Shackleton CR, Pudek M, Erb SR. Indocyanine green clearance as a predictor of successful hepatic resection in cirrhotic patients. Am J Surg 1992;163:515-8.
28. Kim SU, Kim YC, Choi JS, Kim KS, Choi GH, Choi JS, Park JY, Kim DY, Ahn SH, Choi EH, Park YN, Chon CY, Han KH, Kim MJ. Can preoperative diffusion-weighted MRI predict postoperative hepatic insufficiency after curative resection of HBV-related hepatocellular carcinoma? A pilot study. Magn Reson Imaging 2010;28:802-11.
29. Stockmann M, Lock JF, Riecke B, Heyne K, Martus P, Fricke M, Lehmann S, Niehues SM, Schwabe M, Lemke AJ, Neuhaus P. Prediction of postoperative outcome after hepatectomy with a new bedside test for maximal liver function capacity. Ann Surg 2009;250:119-25.
30. Fazakas J, Mándli T, Ther G, Arkossy M, Pap S, Füle B, Németh E, Tóth S, Járay J. Evaluation of liver function for hepatic resection. Transplant Proc 2006;38:798-800.
31. Calès P, Chaigneau J, Hunault G, Michalak S, Cavaro-Menard C, Fasquel JB, Bertrais S, Rousselet MC. Automated morphometry provides accurate and

reproducible virtual staging of liver fibrosis in chronic hepatitis C. J Pathol Inform 2015;6:20.
32. Breit HC, Vosshenrich J, Heye T, Gehweiler J, Winkel DJ, Potthast S, Merkle EM, Boll DT. Assessment of hepatic function employing hepatocyte specific contrast agent concentrations to multifactorially evaluate fibrotic remodeling. Quant Imaging Med Surg 2023;13:4284-94.

Cite this article as: Yu QJ, Luo YC, Zuo ZW, Xie C, Yang TY, Wang T, Cheng L. Utility of gadoxetate disodium-enhanced magnetic resonance imaging in evaluating liver failure risk after major hepatic resection. Quant Imaging Med Surg 2024;14(5):3731-3743. doi: 10.21037/qims-23-1504

